Field-induced first-order antiferromagnetic-ferromagnetic transitions in RMn2Ge2 compounds and their relation to the magnetostriction of the Mn sublattice

Brabers, J.H.V.J.; Buschow, K.H.J.; de Boer, F.R.

Published in:
Physical Review B

Field-induced first-order antiferromagnetic-ferromagnetic transitions in $R\mathrm{Mn_2Ge_2}$ compounds and their relation to the magnetostriction of the Mn sublattice

J. H. V. J. Brabers,* K. H. J. Buschow, and F. R. de Boer
Van der Waals-Zeeman Institute, University of Amsterdam, 1018 XE Amsterdam, The Netherlands
(Received 27 July 1998)

A model for field-induced first-order antiferromagnetic-ferromagnetic transitions is presented. The model is based on a free-energy expression including Mn-Mn and R-Mn exchange interactions, as well as harmonic and anharmonic contributions to the lattice deformation energy. The Mn-Mn interaction is assumed to be linearly dependent on the unit-cell dimensions, giving rise to magnetostrictive phenomena. The magnetostriction appears to be crucial for the occurrence of the first-order antiferromagnetic-ferromagnetic transitions. From the model, an expression for the critical field B_c, corresponding to the first-order transition, has been obtained and used for a description of the temperature dependence of B_c. The model is tested experimentally by magnetization measurements on several $\mathrm{Sm_{1-y}}R_y\mathrm{Mn_2Ge_2}$ compounds and appears to give a good description of the measured B_c vs T relations. Implications of the present work for magnetoresistance in bulk compounds and thin films are briefly discussed. [S0163-1829(99)13113-8]

INTRODUCTION

In the past decade, a lot of research effort has gone into the study of magnetic properties of R-Mn intermetallics. Especially the relation between phase transitions from antiferromagnetism to ferromagnetism and magnetoresistance effects in the layered $R\mathrm{Mn_2Ge_2}$ compounds is an intriguing case in this respect.[1–3] The antiferromagnetic-ferromagnetic transitions in these materials basically involve a transition from a configuration with an antiparallel orientation of the Mn-layer moments to a configuration with a parallel orientation of the Mn-layer moments. Several investigations have made it clear that in many R-Mn compounds, the sign and magnitude of the Mn-Mn interlayer interaction may strongly depend on the Mn-Mn distance.[3,4] For fairly large Mn-Mn distances, the Mn-Mn interlayer interaction is in many compounds ferromagnetic whereas for smaller Mn-Mn distances the interlayer interaction is antiferromagnetic. The distance dependence of the Mn-Mn interlayer interaction is so strong that even slight variations in the unit-cell parameters due to thermal expansion or chemical substitutions are sufficient to modify the interlayer interaction significantly. As a result of this, a compound may undergo a first-order transition from antiferromagnetism to ferromagnetism with increasing temperature. These transitions are likely to be accompanied by an anomaly in the thermal expansion as well as in the electrical resistance.

In an earlier investigation,[3] explicit evidence for a strong distance- (and volume) dependent Mn-Mn interaction was reported. With compounds of the $R\mathrm{Mn_2Ge_2}$ type serving as a model system, it was shown through experiment that in these compounds the Mn-Mn interlayer interaction (n) is strong and scales linearly with the unit-cell volume (ω) and, above 100 K, also with temperature:

$$n = n_0 + n_\omega \omega = a + bT. \tag{1}$$

In this expression for n, which is basically *phenomenological*, n_0 can be viewed upon as the value of the Mn-Mn interlayer-interaction constant at $T=0$. The constants n_ω, a, and b however, cannot be discussed straightforwardly in terms of simple physical concepts and merely represent a set of empirical parameters. A purely theoretical justification for this expression, as well as a numerical evaluation of n_ω, a, and b, would be rather tedious and can in fact only be achieved by evaluation of the Mn-Mn interlayer interaction through rigorous (*ab initio*) calculations of the electronic structure for a whole range of unit-cell dimensions. However, when just taken as an experimental fact, Eq. (1) can be quite useful, as shown in Ref. 3, for instance, in connection to a (mean-field) analysis of temperature-induced antiferromagnetic-ferromagnetic transitions.

In many R-Mn intermetallics, including a lot of $R\mathrm{Mn_2Ge_2}$ compounds, a situation occurs where $n_0, a > 0$ and $n_\omega, b < 0$. As a consequence $n > 0$ for smaller unit-cell volumes or at low temperatures, leading to antiferromagnetism in these cases. When the unit-cell volume becomes larger, for instance through thermal expansion, n decreases and a (temperature-induced) transition to a ferromagnetic state may take place.

Besides temperature-induced antiferromagnetic-ferromagnetic transitions, there is also the possibility of field-induced antiferromagnetic-ferromagnetic transitions. From the point of view of possible sensor applications these latter transitions are much more interesting than the former. Due to the combination of thermal expansion and the volume-dependent Mn-Mn interaction, the critical fields corresponding to these transitions can be strongly dependent on temperature. It may be clear that for applications a thorough understanding of the underlying mechanisms that rule the temperature dependence of the critical fields, is crucial. The aim of this paper is to provide a simple theoretical basis, clarifying the origin and nature of field-induced antiferromagnetic-ferromagnetic transitions in R-Mn systems. The analysis in terms of a simple model is restricted to the case where the Mn sublattice orders at low temperature as a collinear antiferromagnet. This situation occurs in many

of the $R\mathrm{Mn_2Ge_2}$ compounds which will therefore be used as an experimental test case for the model.

THEORETICAL OUTLINE

Field-induced antiferromagnetic-ferromagnetic transitions

In the approach outlined here, the $3d$ moments (Mn) are considered to be independent of temperature, whereas the R-sublattice moments are paramagnetic and therefore strongly temperature dependent. As a consequence, the contribution of the $3d$-sublattice moments $\mathbf{m}_1$ and $\mathbf{m}_2$ to the total magnetic free energy consists only of an exchange term $F_{\mathrm{ex}}^{3d-3d}=n\mathbf{m}_1\cdot\mathbf{m}_2$ and a Zeeman term $F_z^{3d}=-B(\mathbf{m}_1+\mathbf{m}_2)$. The term $-TS_{3d}$ related to the entropy of the $3d$ sublattice can be ignored, as it is a constant because the $3d$ moments are considered to be fixed. The free-energy contribution of the temperature-dependent R sublattice moment, however, does include an entropy-related contribution that varies with temperature, in addition to the contributions from the R-$3d$ exchange and the Zeeman interaction. The total R-sublattice contribution to the free energy F_R can easily be expressed in terms of the effective field $B_R=(-n_{R-3d}|\mathbf{m}_1+\mathbf{m}_2|+B)$, acting on the R sublattice, through application of the identities:

$$m_R=-\frac{\partial F_R}{\partial B_R}\Rightarrow F_R=-\int m_R\,dB_R. \tag{2}$$

For the paramagnetic R sublattice, m_R is described by the Curie law so that

$$m_R=\chi_R B_R=\frac{c_R}{T-\theta}B_R, \tag{3}$$

where

$$c_R=\frac{N_R\mu_{\mathrm{eff}}^2}{3k}. \tag{4}$$

Combining Eqs. (2) and (3) we then have

$$F_R=-\frac{c_R(-2n_{R-3d}|\mathbf{m}_1+\mathbf{m}_2|+\mathbf{B})^2}{2(T-\theta)}. \tag{5}$$

For the formulation of the total free-energy expression, the $3d$-sublattice moments are split into an antiferromagnetic (staggered) component m_Q and a ferromagnetic (uniform) component m_0, so that $|\mathbf{m}_1+\mathbf{m}_2|=2m_0$. The Mn-Mn interlayer exchange energy can, in the lowest order approximation, be represented by a quadratic expansion in the uniform and staggered magnetization components. Neglecting (usually weak) $3d$-anisotropy effects, the total free energy then takes the form:

$$F=-nm_Q^2+nm_0^2+\frac{1}{2}b\omega^2+\phi\omega-2Bm_0$$
$$-\frac{c_R}{2(T-\theta)}(4n_{R-3d}^2m_0^2-4n_{R-3d}m_0B+B^2), \tag{6}$$

where the term $\frac{1}{2}b\omega^2$ represents the harmonic and $\phi\omega$ represents the anharmonic contributions to the deformation energy of the material. The term ω represents the unit-cell volume increase due to thermal expansion and magnetostriction, b is the compressibility and ϕ is the Grüneisen function. At this point, a few remarks should be made. A treatment of the lattice deformation in terms of the unit-cell volume is basically only correct for crystals of cubic symmetry. As the $R\mathrm{Mn_2Ge_2}$ compounds have a tetragonal symmetry, a modified approach would be more appropriate. The antiferromagnetic-ferromagnetic transitions are mainly due to a change of the interlayer interaction constant with changing dimensions of the c axis. A modified free-energy term based on a series expansion in the lattice dimensions, would then contain terms $B_{ij}x_ix_j$ instead of $1/2b\omega^2$ and a term $\phi'_{i,j}x_{i,j}$ instead of $\phi\omega$, where x_i,x_j stand for the length of the a and c axis, respectively. The parameters ϕ and ϕ' are different but depend on the temperature in a similar way. The terms $B_{i,j}$ are proportional to the stiffness constants of the material, which form a tensor, and should not be interpreted as an ''overall'' bulk modulus. The contribution to the Mn-Mn interlayer interaction due to nearest-neighbor interactions between ionic moments on adjacent layers, is expected to scale predominantly with the length of the c axis. The next-nearest-neighbor contribution scales with variations of both the a and the c axis. The empirical relationship with the unit-cell volume revealed by experiment[3] is probably due to the fact that the lengths of the a and c axes scale with temperature in a similar way. Therefore, it seems reasonable to assume, in a lowest-order approximation, a linear relation between the interlayer interaction and the length of both crystal axes: $n=n_0+n_ix_i+n_jx_j$. At higher temperatures, this leads to a linear relation between n and T due to thermal expansion. For cubic crystal symmetries, the equilibrium volume ω corresponds to vanishing of pressure: $p=-\partial F/\partial\omega=0$, whereas for layered tetragonal structures the equilibrium values of $x_{i,j}$ corresponds to vanishing of the stress component along the crystal axes: $\sigma_{i,j}=-\partial F/\partial x_{i,j}=0$. An important observation is the mathematical equivalence of the problems of antiferromagnetic-ferromagnetic transitions in cubic crystals and layered tetragonal compounds, which can be proved easily through some algebra. With appropriate replacement for $\omega(\rightarrow x_i,x_j)$ and $p(\rightarrow\sigma_{i,j})$, the results for cubic symmetries are directly transferable to layered tetragonal systems. To remain in line with a previous paper[3] and for the sake of simplicity, we will outline the approach based on volume expansions ω in the forthcoming part of this section, which yields results of direct relevance to antiferromagnetic-ferromagnetic transitions in cubic systems, with (of course) nonuniaxially arranged ions. We keep in mind however, that the results are also relevant to $R\mathrm{Mn_2Ge_2}$ compounds where the Mn ions are stacked along the c axis and which will serve as a test case for the model described in this section.

The $3d$-sublattice moments are considered to be independent of the applied field B and, in a Heisenberg approach, also independent of the orientation of the sublattice moments. The staggered and uniform components of the $3d$-sublattice magnetizations can then be related to the saturated $3d$-sublattices magnetization: $m_Q^2+m_0^2=m_s^2$. The free-energy expression can than be rearranged as

$$F=2(n-\chi_R n_{R-3d}^2)m_0^2+\frac{1}{2}b\omega^2+\phi\omega$$

$$-2(1-\chi_R n_{R-3d})Bm_0-\frac{\chi_R}{2}B^2-nm_s^2. \tag{7}$$

The equilibrium state corresponds to values of m_0 and ω for which this free-energy expression takes a minimum.

The demand that F takes a minimum with respect to the volume ω, i.e., $(\partial F/\partial\omega)=0$, leads to an expression for ω in terms of the uniform magnetization component m_0:

$$\frac{\partial F}{\partial\omega}=2n_\omega m_0^2-n_\omega m_s^2+b\omega+\phi=0$$

$$\Rightarrow\omega=-\kappa(2n_\omega m_0^2-n_\omega m_s^2+\phi), \tag{8}$$

where κ stands for the compressibility $1/b$ and n_ω for $\partial n/\partial\omega$.

As may be inferred from Eq. (7), the problem of minimizing the free energy with respect to m_0 is mathematically equivalent to that of two $3d$ sublattices interacting with an applied field B' and subject to a mutual interaction corresponding to a coupling constant n':

$$B'=(1-\chi_R n_{R-3d})B, \tag{9a}$$

$$n'=(n-\chi_R n_{R-3d}^2). \tag{9b}$$

One should keep in mind that B' and n' are mathematical rather than physical identities, providing only a convenient description of the $3d$ sublattice. Great care should be taken with respect to conclusions, based on the sign and/or magnitude of B' and n', about the actual physical fields to which the $3d$ sublattice is subjected and which consist of both the applied magnetic field and exchange fields. The relevant free-energy expression, obtained from Eq. (7), can now be expressed as

$$F=2n'm_0^2-2B'm_0+\frac{1}{2}b\omega^2+\phi\omega-nm_s^2. \tag{10}$$

In this expression, the physically unimportant (constant) term $(-\chi_R/2)B^2$ has been left out. However, for an appropriate analysis of the role of the volume magnetostriction in the antiferromagnetic-ferromagnetic transitions, the term $-nm_s^2$ should be kept in the free-energy expression, as the coupling constant n is volume dependent (note that the coupling constant n is indicated, not n'), and the volume in the antiferromagnetic state differs from the volume in the ferromagnetic state. Keeping in mind that the uniform magnetizations (m_0) of the ferromagnetic and antiferromagnetic states are different, the latter statement can be easily verified through inspection of Eq. (8).

In the ferromagnetic state, the equilibrium value of m_0 is simply the saturated $3d$-sublattice value m_s. For the (canted) antiferromagnetic state, application of the condition $(\partial F/\partial m_0)=0$ yields the equilibrium value for m_0:

$$m_0=\frac{B'}{2n'}=\frac{1-\chi_R n_{R-3d}}{2(n-\chi_R n_{R-3d}^2)}B. \tag{11}$$

By substitution of the expression for the uniform magnetization into Eqs. (8) and (10), the free energy for the ferromagnetic as well as for the antiferromagnetic state can be expressed in terms of the field B'. After some rearrangements we have for the antiferromagnetic state

$$F_{\mathrm{AF}}=\frac{n_\omega^2\kappa}{8n_{\mathrm{AF}}'^4}B'^4-\left(\frac{n_\omega^2\kappa m_s^2}{2n_{\mathrm{AF}}'^2}+\frac{1}{2n_{\mathrm{AF}}'}\right)B'^2$$
$$+\frac{1}{2}n_\omega^2\kappa m_s^4-\frac{1}{2}\kappa\phi^2-n_{\mathrm{AF}}m_s^2, \tag{12}$$

and for the ferromagnetic state

$$F_{\mathrm{F}}=2n_{\mathrm{F}}'^2m_s^2-2m_sB'+\frac{1}{2}\kappa n_\omega^2m_s^4-\frac{1}{2}\kappa\phi^2-n_{\mathrm{F}}m_s^2. \tag{13}$$

Disregarding hysteresis effects (which are supposed to determine the position of the critical fields only to a minor extent), the transition between the antiferromagnetic and the ferromagnetic state is simply supposed to take place at a field B_c' for which $F_{\mathrm{AF}}=F_{\mathrm{F}}$, that is when

$$F_{\mathrm{AF}}-F_{\mathrm{F}}=\frac{n_\omega^2\kappa}{8n_{\mathrm{AF}}'^4}B_c'^4-\left(\frac{n_\omega^2\kappa m_s^2}{2n_{\mathrm{AF}}'^2}+\frac{1}{2n_{\mathrm{AF}}'}\right)B_c'^2+2m_sB_c'$$
$$-(n_{\mathrm{AF}}+2n_{\mathrm{F}}'-n_{\mathrm{F}})m_s^2=0. \tag{14}$$

The term $-n_{\mathrm{AF}}m_s^2-2n_{\mathrm{F}}'m_s^2+n_{\mathrm{F}}m_s^2$ can be rearranged by using expression (9b) for n':

$$(-n_{\mathrm{AF}}-2n_{\mathrm{F}}'+n_{\mathrm{F}})m_s^2=-(n_{\mathrm{AF}}'+n_{\mathrm{F}}')m_s^2. \tag{15}$$

For convenience we express the coupling constants n_{F} and n_{F}' in terms of the coupling constants for the antiferromagnetic state n_{AF} and n_{AF}', respectively. Both n_{F} and n_{AF} depend on the volume corresponding to the respective states to which they refer. By introduction of the volumes ω_{F} and ω_{AF} for the antiferromagnetic and ferromagnetic state, respectively, Eq. (8) and the relation $n=n_0+n_\omega\omega_{\mathrm{AF,F}}$ enable us to relate n_{F} to n_{AF}:

$$n_{\mathrm{F}}=n_0+n_\omega\omega_{\mathrm{F}}=n_0-n_\omega^2\kappa m_s^2-\phi n_\omega\kappa,$$

$$n_{\mathrm{AF}}=n_0+n_\omega\omega_{\mathrm{AF}}=n_0-\frac{n_\omega^2\kappa}{2n_{\mathrm{AF}}'^2}B'^2+n_\omega^2\kappa m_s^2-\phi n_\omega\kappa. \tag{16}$$

Analoguous expressions hold for n_{AF}' and n_{F}' so that

$$n'_{\mathrm{AF}}=n'^{B'=0}_{\mathrm{AF}}-\frac{n_\omega^2\kappa}{2n'^2_{\mathrm{AF}}}B'^2,$$

$$n'_{\mathrm{F}}=n'^{B'=0}_{\mathrm{AF}}-2n_\omega^2\kappa m_s^2,$$

$$-(n'_{\mathrm{AF}}+n'_{\mathrm{F}})=-\left(2n'^{B'=0}_{\mathrm{AF}}-2n_\omega^2\kappa m_s^2-\frac{n_\omega^2\kappa}{2n'_{\mathrm{AF}}}B'^2\right). \tag{17}$$

Combining the lower expression with Eqs. (14) and (15), n'_{F} can now be removed from the condition for the antiferromagnetic-ferromagnetic transition, which then reads

$$\frac{n_\omega^2\kappa}{8n'^4_{\mathrm{AF}}}B_c'^4-\frac{1}{2n'_{\mathrm{AF}}}B_c'^2+2m_sB'_c-(2n'^{B'=0}_{\mathrm{AF}}-2n_\omega^2\kappa m_s^2)m_s^2=0. \tag{18}$$

From this equation we see that the critical field B'_c is the solution of a fourth-order polynomial equation, which cannot easily be solved algebraically. In practice however, the field B' is often of the order of only a few teslas, the term $n_\omega^2\kappa$ rather modest and the effective coupling constant n'_{AF} fairly large. Therefore, the fourth-order term in the polynominal is negligible as it is a few orders of magnitude smaller than for instance the second-order term.

Furthermore, inspection of the upper expression in the set of equations (17) shows that under the same conditions that make the fourth-order term in Eq. (17) negligibly small, n'_{AF} is almost equal to $n'^{B'=0}_{\mathrm{AF}}$. Resuming we may therefore conclude that in a fairly good approximation, the critical field B'_c can be expressed as the solution of a second-order polynomial equation:

$$F_{\mathrm{AF}}-F_{\mathrm{F}}\approx-\frac{1}{2n'_{\mathrm{AF}}}B_c'^2+2m_sB'_c-(2n'_{\mathrm{AF}}-2n_\omega^2\kappa m_s^2)m_s^2\approx0, \tag{19}$$

the solutions of which can be expressed as

$$B'_c=2n'_{\mathrm{AF}}m_s\mp2n'_{\mathrm{AF}}m_s^2\sqrt{\frac{n_\omega^2\kappa}{n'_{\mathrm{AF}}}}. \tag{20}$$

This expression incorporates all relevant aspects of the antiferromagnetic-ferromagnetic transitions, which will be subsequently discussed below.

First we discuss the case where magnetostrictive effects are absent, i.e., $n_\omega=0$, and $n'_{\mathrm{AF}}=n'_{\mathrm{F}}=n'$.

In the absence of magnetostrictive effects, no *first-order* transitions from antiferromagnetism to ferromagnetism occur. The magnetization process consists of a gradual bending of the $3d$-sublattice vectors towards the applied-field direction. As may be inferred from Eq. (11), the magnetization is related to the applied field as $m=2m_0=B'/n'_{\mathrm{AF}}$. As may be inferred from Eq. (20), the condition $F_{\mathrm{F}}=F_{\mathrm{AF}}$, for the transition from a canted (antiferromagnetic) configuration to a ferromagnetic state, yields only a single solution $B'_0=2n'_{\mathrm{AF}}m_s$ corresponding to a second-order transition, marking the completion of a bending process. For B' values exceeding B'_0 the (canted) antiferromagnetic state is unstable.

In the case where the constituent R component is magnetic, the field B'_0 and the coupling constant n'_{AF} are given by Eqs. (9a) and (9b), respectively. When the R component is nonmagnetic, the field B'_0 is simply equal to the applied field and the effective coupling constant n'_{AF} has to be replaced by the exchange parameter n_{AF}.

When magnetostrictive behavior is present ($n_\omega\neq0$) however, Eq. (20) yields two solutions B'_1 and B'_2:

$$B'_{1,2}=B'_0\mp2n'_{\mathrm{AF}}m_s^2\sqrt{\frac{n_\omega^2\kappa}{n'_{\mathrm{AF}}}}. \tag{21}$$

Equation (19) shows that for $B'<B'_1$ the free-energy difference $F_{\mathrm{AF}}-F_{\mathrm{F}}<0$, so that the canted antiferromagnetic state is stable in this regime. The field B'_1 marks the discontinuous transition ($F_{\mathrm{AF}}=F_{\mathrm{F}}$) to the ferromagnetic state corresponding to a field regime where $F_{\mathrm{AF}}-F_{\mathrm{F}}>0$. It is stressed that this transition is fully due to the presence of magnetostrictive effects. The magnetostriction favors the ferromagnetic state, as it gives rise to a lower volume contribution to the total free energy than the antiferromagnetic state. In this respect, magnetostriction enhances the effect of the Zeeman energy which also favors the ferromagnetic state. The result is a first-order transition due to a ''crossing'' of the respective F_{AF} vs B' and the F_{F} vs B' curves at the field B'_1. The field $B'_2>B'_0$ has no physical relevancy, as it exceeds the field B'_0 at which even in a continuous bending process the (canted) antiferromagnetic alignment would transform into the ferromagnetic state.

Resuming the above, we conclude that field-induced antiferromagnetic-ferromagnetic transitions of first order can be explained on the basis of magnetostriction, and that the corresponding critical fields B' can be expressed in terms of the (volume-dependent) exchange-coupling constants [$n=n(\omega),n_{R-3d}$], the compressibility κ, the R susceptibility χ_R, and the saturation moment m_s of the $3d$ sublattice. Using Eq. (9a), the critical effective field B'_1 can be related to a critical value of the applied field B_c. An analysis of the effect of temperature on the critical applied field B_c marking the transition is straightforward.

Due to thermal expansion, the volume-dependent coupling constant n depends indirectly on the temperature. Within the theoretical frame of this paper, thermal expansion is determined exclusively by and proportional to the Grüneisen function $\phi(T)$, as can be verified by inspection of Eq. (8). At temperatures above 100 K, the Grüneisen function is approximately a linear function of temperature, and therefore $n=n_0+n_\omega\omega$ is also a linear function of temperature: $n=a+bT$.

Using Eqs. (2), (9a), and (9b), an expression for B_c involving temperature reads

$$B_c=\frac{2n'_{\mathrm{AF}}m_s-2n'_{\mathrm{AF}}m_s^2\sqrt{n_\omega^2\kappa/n'_{\mathrm{AF}}}}{1-[c_R/(T-\theta)]n_{R-3d}}=\frac{2\{a+bT-[c_R/(T-\theta)]n_{R-3d}^2\}\{m_s-m_s^2\sqrt{n_\omega^2\kappa/[a+bT-[c_R/(T-\theta)]n_{R-3d}^2]}\}}{1-[c_R/(T-\theta)]n_{R-3d}}. \tag{22}$$

To have some idea about the effect of each material parameter on B_c, typical curves of the critical field as a function of temperature are presented in Figs. 1(a)–1(d) for different choices of the parameters a, b, c, and $n_\omega^2\kappa$. The parameter values c_R, m_s, and θ and $n_{R\text{-Mn}}$ have been chosen such that they match closely to the values for the $SmMn_2Ge_2$ related compounds. The order of magnitude of a, b, and $n_\omega^2\kappa$ is taken in accordance with the experimental results for $SmMn_2Ge_2$-based compounds to be presented later in this paper. Each figure corresponds to a calculation for which only a single parameter was varied around its typical value in the $SmMn_2Ge_2$-based compounds, whereas all other parameters were kept at a fixed value in the calculation. Trends in the position of the individual curves with increasing values of the varying parameter are schematically indicated by the arrow in each figure.

Figure 1(a) shows the critical field as a function of temperature for various choices of a. As expected, the critical field tends to increase with increasing a: with increasing a, the value of the Mn-Mn interaction constant $n_{\mathrm{AF}}=a+bT$ becomes larger at a particular temperature, making the (canted) antiferromagnetic state more and more stable compared to the ferromagnetic state so that the critical field becomes larger.

Figure 1(b) illustrates the effect of b (the variation of the Mn-Mn interlayer coupling with temperature) on the value of B_c. In many R-Mn intermetallics $b<0$ so that with increasing temperature the Mn-Mn interlayer interaction decreases. With decreasing b, n_{AF} tends to decrease more and more rapidly with increasing temperature, so that the antiferromagnetic state becomes less stable. As a logical consequence, B_c therefore drops steeply with decreasing b.

Whereas the parameters a and b primerily affect the order of magnitude of the critical field, the Curie constant c_R of the R sublattice has also a clear effect on the shape of the B_c vs T curve. This is clearly illustrated in Fig. 1(c). As may be inferred from Eqs. (9a) and (9b), the magnetic R sublattice has a dual effect. Firstly it tends to increase or decrease (depending on the sign and magnitude of $\chi_R n_{R\text{-Mn}}$) the effective field experienced by the Mn sublattice, respectively, enhancing the polarization (canting) or the depolarization of the Mn-sublattice moments. A second effect is a decrease of the *effective* coupling constant n'_{AF} [see Eq. (9b)], making the (canted) antiferromagnetic configuration less stable. Figure 1(c) is based on a calculation in which $n_{R\text{-Mn}}>0$, i.e., a case where the R-Mn exchange field lowers the effective field. Apparently, however, this effect is suppressed by the decrease of n'_{AF} so that the overall effect of a magnetic R sublattice consists of a decrease of the critical field. This effect can be clearly observed in Fig. 1(c): with increasing c_R, the critical field at a particular temperature decreases. With increasing temperature however, the role of the paramagnetic R sublattice becomes less important [$\chi_R=c_R/(T-\theta)$ decreases], and the relation between B_c and T becomes dominated more and more by the temperature dependence of $n_{\text{Mn-Mn}}=a+bT$. Although only slightly visible in Fig. 1(c), all the curves tend to converge to a common line at higher temperatures. For sufficiently large c_R, the interplay between the temperature dependence of the R susceptibility χ_R and $n_{\text{Mn-Mn}}$ gives rise to a maximum in the B_c vs T curve. This maximum becomes sharper as c_R increases.

Inspection of Eq. (22) shows that the magnetostriction and the compressibility enter the expression for the critical field through a single, common parameter $n_\omega^2\kappa$. This parameter affects the overall magnitude of the critical fields rather

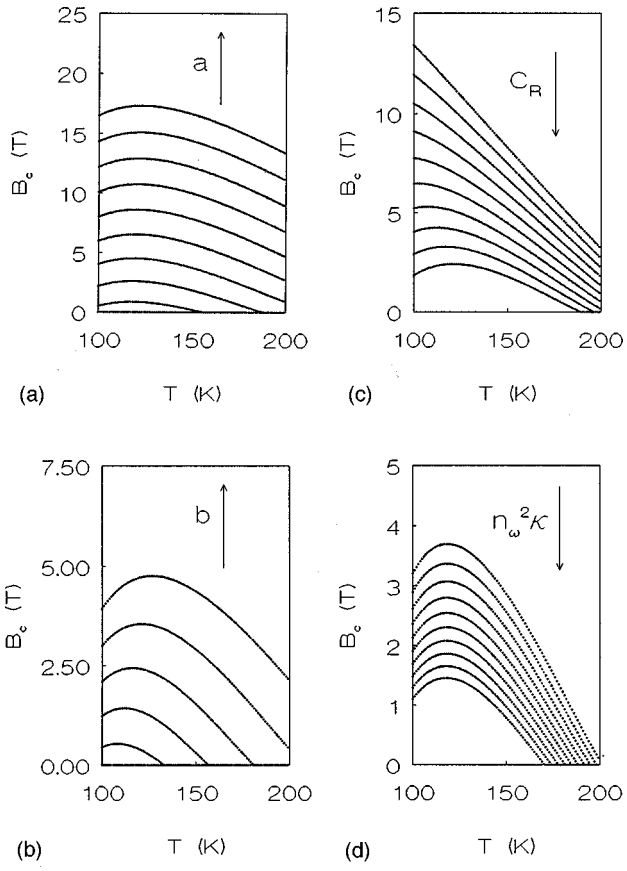

FIG. 1. (a)–(d) Influence of the parameters a, b, $n_\omega^2\kappa$, and c_R on the critical field. The individual figures correspond to a series of calculations of B_c vs T, varying only a single parameter around a certain value and the others are kept constant. The input values of the parameters when held constant are $a=12$ Tf.u./μ_B, $b=-0.05$ Tf.u./μ_B K, $n_{R-3d}=-55$ Tf.u./μ_B, $n_\omega^2\kappa=0.2$ T/μ_B^3, $c_R=0.126\,\mu_B$ K. When varied, the parameters are chosen within an interval around these values (9.6 Tf.u./$\mu_B\leqslant a\leqslant 19.6$ Tf.u./μ_B, -0.0875 Tf.u./μ_B K$\leqslant b\leqslant -0.0375$ Tf.u./μ_B K, $0\leqslant c_R\leqslant 0.122\mu_B$ K, 0.2 T/$\mu_B^3\leqslant n_\omega^2\kappa\leqslant 0.8$ Tμ_B^3). The effect of an increase of a particular parameter is schematically indicated by the arrow.

than the shape of the B_c vs T curve and the position of the maximum herein. When $n_\omega^2\kappa$ increases, the critical field tends to decrease. This is, in fact, what one would expect intuitively as both an increase of the compressibility κ as well as the volume dependence of the Mn-Mn interlayer interaction obviously enhance the stabilization of the ferromagnetic state. An increase of κ reduces the lattice-deformation energy necessary to overcome in the antiferromagnetic-ferromagnetic transition, whereas a stronger volume dependence of the interlayer interaction (reflected in the parameter $n_\omega<0$) leads to an increase of the magnetostriction and a decrease of the free-energy connected to the fully parallel (ferromagnetic) alignment of the Mn-sublattice moments.

An interesting byproduct of the analysis of the critical fields is an expression for the critical temperature related to a temperature-induced antiferro-ferro transition in an applied field. By setting $B_c'=0$ in expression (19), the condition for the (first-order) transition in zero field can be obtained straightforwardly:

$$n_{\mathrm{AF}}'-n_\omega^2\kappa m_s^2=0. \tag{23}$$

With a linear relation between $n_{\mathrm{AF}}'=a+bT$, the critical temperature T_c, marking the transition, can be expressed as

$$T_c=\frac{1}{b}(n_\omega^2\kappa m_s^2-a). \tag{24}$$

The parameter a, being the zero-temperature offset of the coupling constant, differs for each compound and depends strongly on the unit-cell dimensions. Variations of the unit-cell dimensions ω_s, due to chemical substitutions on the R or metalloid sublattices, affect the parameter a in a similar way as the volume changes ω due to magnetization of the sample and/or thermal expansion. Analogous to the relation $n=n_0+n_\omega\omega$, we thus have a relation $a=a_0+a_\omega\omega_s$. By direct substitution of this expression in Eq. (23) it can be seen that a linear relation exists between T_c and the unit-cell volume (ω_s). This result is consistent with theory and experiments reported in a previous investigation[3] devoted to the effect of temperature on the type of magnetic ordering in R-Mn compounds. But, although based on almost the same theoretical concepts as the present investigation, the expression for T_c given in Ref. 3 is more complicated than Eq. (23) and obtained in a less straightforward way. Straightforward use of Eq. (19) allows an extension of Eq. (23) incorporating the effect on nonzero applied fields on T_c.

Paramagnetic Sm sublattices

As in the forthcoming sections the model outlined above will be verified on the basis of magnetization measurements on $Sm_{1-x}R_xMn_2Ge_2$ compounds, some considerations about the paramagnetic state of the Sm sublattice in these compounds are justified here.

The energy difference between the ground-state $J=5/2$ multiplet and the $J=7/2$ multiplet, being the first excited state of Sm, is relatively small and therefore intermixing of the $J=5/2$ and $J=7/2$ multiplets takes place already at temperatures close to room temperature. As a result, the inverse susceptibility of Sm sublattices in the paramagnetic state does not show over the entire temperature range Curie-Weiss behavior corresponding to the paramagnetic state. Only at lower temperatures Curie-Weiss behavior may occur. To illustrate this, Fig. 2 shows a calculation (drawn curve) of the inverse susceptibility (defined as B/M) of a Sm sublattice in a field $B=150$ T, taking intermixing between the $J=5/2$ state and the $J=7/2$ state into account ($E_{J=7/2}-E_{J=5/2}=1340$ K). No Sm-Sm interaction or crystal-field effects were taken into account in the calculation. The dashed line in Fig. 2 represents the inverse susceptibility, based on the $J=5/2$ multiplet only, according to Curie's law.

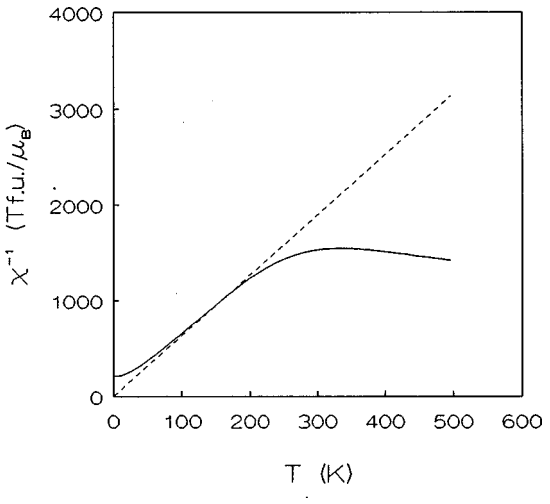

FIG. 2. Calculated inverse susceptibility of a paramagnetic Sm sublattice (solid curve) taking intermixing of $J=5/2$ and $J=7/2$ states into account and inverse susceptibility according to Curie-Weiss (dashed curve) based on the $J=5/2$ multiplet only. The solid curve was calculated under the assumption of a magnetic field of 150 T, a value typical for the R-Mn exchange field acting on the R sublattice in $SmMn_2Ge_2$.

Between 100 and 200 K both curves almost coalesce. Therefore, the application of a Curie-Weiss law to the Sm sublattices still seems a reasonable procedure in this temperature regime. In connection to this, it is worth mentioning that, according to additional calculations, the introduction of crystal-field effects or Sm-Sm interactions does not impose a different point of view in this respect. An important implication of Fig. 2 is that on the basis of $Sm_{1-y}R_yMn_2Ge_2$ compounds a test of the model outlined previously is only possible at temperatures between 100 and 200 K.

EXPERIMENT

In order to verify the applicability of the model outlined above, we will check whether it is possible to reproduce the experimentally obtained values of the critical field for several RMn_2Ge_2 compounds. Polycrystalline specimens of these compounds were prepared by arc melting and subsequent annealing at 800 °C. The quality of the samples was verified by x-ray diffraction: all samples were found to be approximately single phase ($ThCr_2Si_2$ structure). Magnetization measurements both as a function of temperature and field were performed on a superconducting quantum interference device magnetometer (Quantum Design).

RESULTS AND DISCUSSION

Test of the model

Among the $R\mathrm{Mn_2Ge_2}$ compounds there are a lot of compounds in which, in a particular temperature regime, the Mn sublattice is subject to an antiferromagnetic interaction, whereas the R sublattice is paramagnetic. Examples of such compounds are for instance $\mathrm{GdMn_2Ge_2}$ and some $\mathrm{Sm_{1-x}}R_x\mathrm{Mn_2Ge_2}$ compounds.[6] The latter compounds exhibit a phenomenon known as reentrant ferromagnetism. At low temperatures, the compound is ferromagnetic due to ordering of both the R and Mn sublattices. At a certain temperature T_1, the order of the R sublattice collapses and an antiferromagnetic Mn sublattice remains up to a higher temperature T_2 at which the system undergoes another phase transition towards ferromagnetism. This latter transition does not involve, however, a reentering of the magnetic ordering on the R sublattice which remains paramagnetic. The exact values of T_1 and T_2 in the $\mathrm{Sm_{1-x}}R_x\mathrm{Mn_2Ge_2}$ compounds depend on R and its concentration x. In the compound $\mathrm{GdMn_2Ge_2}$, a change from ferromagnetism to antiferromagnetism occurs at 100 K, and above this temperature the Gd sublattice is paramagnetic. The ordering temperatures of the Mn sublattice in various $R\mathrm{Mn_2Ge_2}$ compounds varies between 350 and 450 K. The antiferromagnetic ordering of the Mn sublattice in these compounds is without exception always of a collinear type and, therefore, the antiferromagnetic $R\mathrm{Mn_2Ge_2}$ compounds provide excellent test cases for the model discussed in the previous section.

An appropriate test of the model will be based on Eq. (22) and consist of a (least-squares) fit of experimentally observed critical fields at various temperatures. The value of such fitting procedures depends largely on the number of fitted material parameters involved which should be kept as low as possible. Under practical conditions, a few of the material parameters involved in the antiferromagnetic-ferromagnetic transition can be obtained from measurements of the magnetization on single crystals as well as on polycrystalline material. For the $R\mathrm{Mn_2Ge_2}$ compounds, values of the microscopic spin-spin coupling constant $J_{R\text{-Mn}}$, corresponding to the R-Mn interaction were obtained by Iwata *et al.*[5] from magnetization measurements on a $\mathrm{PrMn_2Ge_2}$ single crystal ($J_{R\text{-Mn}}/k = 4$ K). Usually the $J_{R\text{-Mn}}$ interaction does not vary significantly through a series of R-3d intermetallics with different R components. Through a simple mean-field analysis[7] the $J_{R\text{-Mn}}$ values can be related to their mean-field equivalent $n_{R\text{-Mn}}$. The saturation moment of the Mn sublattice can be easily obtained from low-temperature magnetization measurements, assuming the rare-earth moments equal to the free-ion moments and the orientation of the R and Mn moments to be either parallel or antiparallel, depending on whether a light or a heavy R element is involved. The value of the Curie constant c_R can be calculated from Eq. (4). The parameters a, b, and $n_\omega^2\kappa$ are, in principle, unknown and may serve as adjustable parameters in a fitting procedure.

Figure 3 shows examples of various magnetization curves measured on $\mathrm{Sm_{0.9}Lu_{0.1}Mn_2Ge_2}$ at different temperatures. The curves correspond to measurements in which the field decreases from 5.5 T to zero. Field-induced transitions from a high-magnetization (ferromagnetic) to a low-magnetization (antiferromagnetic) state appear to occur in a wide temperature range. Clearly recognizable is the effect of temperature on the position of the (first-order) antiferromagnetic-ferromagnetic transitions. Initially, the critical field tends to increase with temperature but at higher temperatures the critical field decreases significantly with temperature. This behavior resembles that observed in several of the calculated curves pictured in Figs. 1(a)–1(d), in particular in those for which the influence of the R sublattice is large, i.e., for the larger Curie constants. A more precise estimate of the temperature dependence of B_c in $\mathrm{Sm_{0.9}Lu_{0.1}Mn_2Ge_2}$ was obtained from magnetization curves similar to those pictured in Fig. 3, identifying the critical field with the field corresponding to the maximum derivative as this is assumed to mark the transition of the bulk cluster in the (due to R substitutions) structurally disordered material. Plotted as a function of temperature, the critical fields obtained from this procedure show a behavior represented in Fig. 4(a). Similar data were obtained on two other samples with, $\mathrm{Sm_{0.9}Y_{0.1}Mn_2Ge_2}$ and $\mathrm{Sm_{0.8}Lu_{0.2}Mn_2Ge_2}$ being their nominal compositions. The respective B_c vs T curves are represented in Figs. 4(a)–4(c).

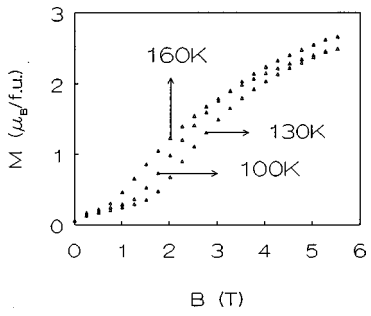

FIG. 3. Magnetization as a function of applied field at the temperatures indicated. The curves correspond to field sweep during which the applied field decreases from 5.5 T down to zero.

Figures 4(a)–4(c) show B_c vs T curves which closely resemble many of the calculated curves pictured in Figs. 1(a)–1(d). Apparently, the influence of the R sublattice is still quite strong at temperatures close to 100 K, as the critical fields increase at these temperatures. After reaching a maximum, the critical fields tend to decrease at higher temperatures and finally become zero. A particular point of interest is the fact that upon going from Fig. 4(a) to Fig. 4(c) the parabola-shaped B_c vs T curves shift downwards. As will be discussed below, this behavior is consistent with the previously outlined model if we consider the dilution rate and unit-cell volume of the specimens corresponding to Figs. 4(a)–4(c).

Most likely the specimens used in this investigation do not have the exact nominal composition chosen by means of the relative amounts of the constituent starting materials before arc-melting. The reason for this is that both Mn and Sm tend to evaporate strongly during the melting process. This explains why it is possible that the specimen with nominal rare-earth composition $R = \mathrm{Sm_{0.9}Y_{0.1}}$ has a smaller unit-cell volume than the specimen with $R = \mathrm{Sm_{0.9}Lu_{0.1}}$, although considerations based on the lanthanide contraction suggest exactly the opposite. Consequently, the magnetic dilution of the R sublattice in the latter sample should be lower than in the first sample, as larger unit-cell volumes require higher Sm concentrations in this particular case (lanthanide contraction). Figures 4(a)–4(c) have been deliberately arranged such

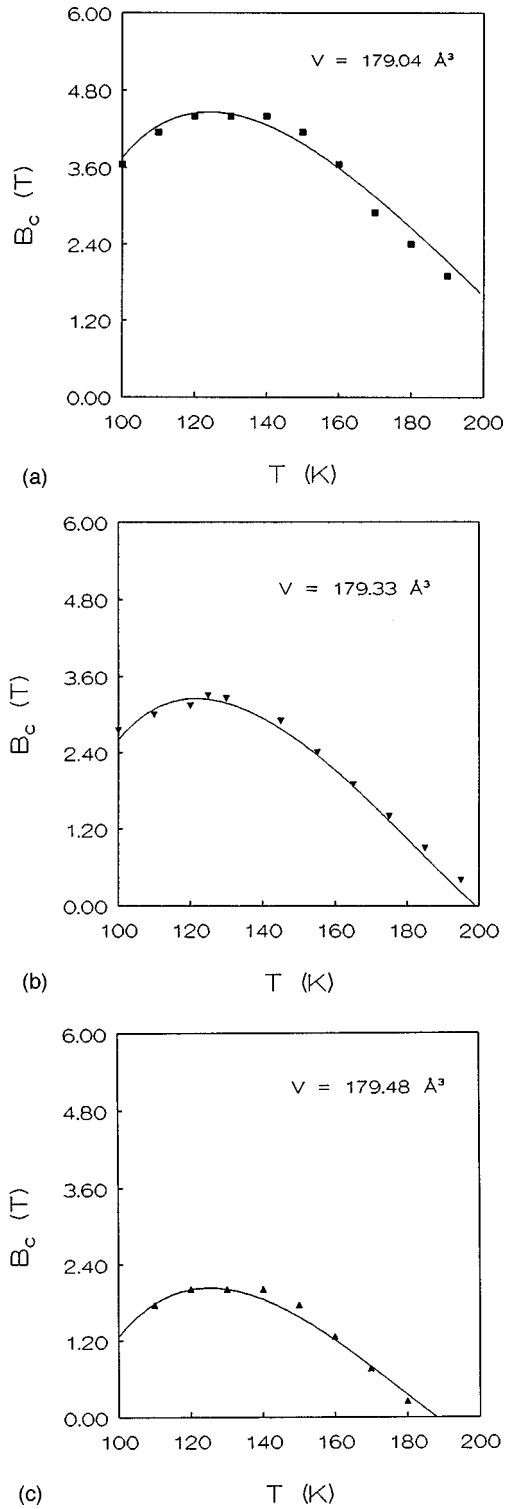

FIG. 4. (a)–(c) B_c vs T curves obtained from measurements of the magnetization as a function of field for three different compounds. Nominal stoichiometries are $Sm_{0.8}Lu_{0.2}Mn_2Ge_2$ (a), $Sm_{0.9}Y_{0.1}Mn_2Ge_2$ (b), $Sm_{0.9}Lu_{0.1}Mn_2Ge_2$ (c). Unit-cell volumes are indicated in each figure. Solid curves: least-squares fits based on Eq. (22).

that the unit-cell volume (at room temperature) of the corresponding specimens decreases when going from Fig. 4(a) to Fig. 4(c) (generally, a volume decrease corresponds to a decrease of both the a and c axes in the particular case of these compounds). Differences in room-temperature volumes are also a good measure for volume differences at lower temperatures as, for instance, clear Invar behavior is absent in the RMn_2Ge_2 compounds. The Mn-Mn interlayer coupling constant can be described by the relation $n=a+bT$, where b is expected to be more or less constant for all specimens and $a>0$ varies for each compound and becomes smaller when the (zero temperature) unit-cell dimensions become smaller. The effect of variations of the parameter a is represented in Fig. 1(a) which shows B_c vs T curves shifting downwards as a decreases. In this respect, the observed shift in Figs. 4(a)–4(c) is in agreement with our model.

The full lines in Figs. 4(a)–4(c) represent the results of least-squares fits based on Eq. (22). As can be seen, the best fitting curves represent the observed critical fields quite well. The parameters a, b, and $n_\omega^2\kappa$ served as adjustable parameters in each calculation procedure, other parameters were fixed input parameters held constant throughout each fitting procedure. For the Curie constants c_R, values based on the nominal compositions were used, although slight deviations from these values occur in the actual samples. For the saturation moment m_s, the value derived from the low-field magnetization measurements at 5 K ($1.4\mu_B$) was assumed for all compounds. The values to be used for the paramagnetic Curie constant are subject to some considerations. The value of θ has to be considered as an intrinsic parameter of the R sublattice related to the R-R interaction only. Therefore, θ should be lower than the actual temperature which marks the collapse of magnetic ordering of the R sublattice, as the latter temperature is also strongly determined by the R-Mn interaction. The fitting procedures were repeated for several values of the paramagnetic Curie temperature θ. For all specimens the θ value giving the best fit is approximately 30 K. It is interesting to mention that this result is consistent with NMR experiments under high pressure performed by Lord *et al.*,[8] suggesting an ''intrinsic'' R-sublattice Curie temperature of approximately the same value.

Due to the fact that the c_R values are not precisely known, as the compositions of the R sublattice may deviate from their nominal values, the best fitting values of a, b, and $n_\omega^2\kappa$ should be taken with some reservation and should be considered as realistic but not as precise estimates. However, it is worth mentioning that the values of the parameter b are of the order of $0.05\,\mathrm{Tf.u.}/\mu_B\,\mathrm{K}$ which is also the case for the YMn_2Ge_2 compound, for which an estimate for b can be obtained from magnetization measurements.[3] The values of the parameter a obtained in the present investigation vary between 12.4 and $13.6\,\mathrm{Tf.u.}/\mu_B$. These values are significantly lower than the value which can be obtained for YMn_2Ge_2 compound as should be expected on basis of the lanthanide contraction. This can be understood easily as follows. Within a series of R-$3d$ intermetallic compounds, the lattice constants of the compounds with $R=\mathrm{Y}$ are usually close to those for the compound with $R=\mathrm{Tb}$. As the atom number of Tb is larger than the atom number of Sm, the lattice parameters for $R=\mathrm{Tb}$ (and also for $R=\mathrm{Y}$) should be smaller than for $R=\mathrm{Sm}$. A consequence of this is that, at a given temperature, the antiferromagnetic Mn-Mn interlayer coupling in $Sm_{1-y}R_yMn_2Ge_2$ compounds where $y\ll 1$ should be much weaker than in YMn_2Ge_2. As the value of b seems to be the same for the cases where $R=\mathrm{Y}$ and R

=Sm, differences in the interlayer coupling strength ($n_{\text{Mn-Mn}}=a+bT$) must be totally accounted for by the value of a, which should decrease in order to have a weaker Mn-Mn interlayer coupling.

Resuming this section we can conclude that the model presented in this paper describes the temperature behavior of the critical fields corresponding to field-induced antiferromagnetic-ferromagnetic transitions very well from a qualitative point of view, whereas very reasonable quantitative results are obtained as well.

Magnetoresistance effects; limitations of the model with respect to its application to magnetic multilayers

Some time ago, several investigations reported the observation of giant magntoresistance (GMR) effects in $SmMn_2Ge_2$ compounds.[1,2] It was suggested that due to the layered arrangement of the Mn layers in this compound an analogy to GMR effects in artificial magnetic multilayer systems exists. In an earlier investigation[3] on temperature-induced antiferromagnetic-ferromagnetic transitions we pointed out that magnetovolume and related Fermi-surface effects are most likely the driving mechanism behind the GMR effects in $SmMn_2Ge_2$-based compounds, instead of spin-dependent scattering, which is often suggested as the cause for GMR in artificial multilayers. This suggestion is consistent with other investigations[1] and corroborated by the investigations reported in the present paper, which clearly show that magnetovolume effects are a basic feature of field-induced antiferromagnetic-ferromagnetic transitions in the compounds under investigation. From this point of view it would be interesting to consider whether the theoretical framework described in this paper also provides an *alternative* interpretation of GMR in metallic multilayer systems [dropping the R contribution to the free-energy expression in Eq. (7) would result in an appropriate free-energy expression for this purpose]. It is, however, very easy to point out that this is simply not the case. The magnetovolume effects necessary for the antiferromagnetic-ferromagnetic transition to take place enter in our model through the distance-dependent interlayer interaction, or more precisely, through its volume derivative. In artificial multilayer systems, the interlayer interaction is of a Ruderman-Kittel-Kasuya-Yosida type and therefore also distance dependent but the magnitude of this interaction and its variation as a function of the interlayer distance or interlayer volume are several orders of magnitude smaller than in many bulk intermetallic compounds. Magnetovolume effects in artificial multilayer systems, being proportional to $n_\omega \kappa m_0^2$ [see Eq. (8)], are therefore also expected to be a few orders of magnitude smaller than their analogs in bulk compounds. With respect to GMR in thin-film metallic multilayers an interpretation in terms of exchange-related magnetovolume effects is therefore inadequate.

CONCLUSIONS

In the present paper a model is outlined which provides a solid interpretation of field-induced antiferromagnetic-ferromagnetic transitions in compounds with a cubic crystal symmetry and compounds with layered arrangements of magnetic ($3d$) ions. The model describes these transitions in terms of volume or distance-dependent exchange interactions and both harmonic and anharmonic contributions to the lattice deformation energy. The existence of a strong distance or volume dependence of the $3d$-$3d$ interaction, leading to magnetovolume effects, appears to be crucial for the occurrence of field-induced first-order antiferromagnetic-ferromagnetic transitions. Assuming a linear relation between unit-cell dimensions and temperature, an expression for the critical fields marking the transitions can be obtained.

Application of the model to RMn_2Ge_2 systems confirms the usefulness of the model. The model provides both a qualitative and quantitative reproduction of B_c curves obtained from magnetization measurements. We can therefore conclude that the nature of the antiferromagnetic-ferromagnetic transitions, being related to the dependence of the $3d$-$3d$ interaction on the unit-cell dimensions, is fairly well understood.

The model provides a possible explanation for the occurrence of GMR effects in $SmMn_2Ge_2$-related compounds but is not fully applicable to thin-film multilayer systems.

Finally, it is worth mentioning that recently a different theoretical approach to antiferromagnetic-ferromagnetic transitions was presented by Hernando *et al.*,[9] based on a ''full itinerant'' treatment of $3d$ moments in terms of the Stoner model. Our model, treating the Mn moments within a Heisenberg formalism and therefore basically as localized, can be considered as more or less complementary to Hernando's model. Volume effects, playing a crucial role in the occurrence of antiferromagnetic-ferromagnetic transitions, are a common feature of both models however. In Hernando's model, the mechanism behind the antiferro-ferro transition is related primarily to the volume dependence of the density of states at the Fermi level, whereas in an approximation based on fixed localized moments like ours, volume effects can enter the model only via the mean-field exchange parameter. A volume-dependent exchange contribution to the free energy is, however, a conceptual similarity between both models. In spite of the predominantly itinerant nature of the Mn moments in the RMn_2Ge_2 compounds, the application of our model to the antiferromagnetic-ferromagnetic transitions in these compounds does not seem to be inappropriate, as for instance, band-structure calculations have shown that for these compounds the magnitude of the Mn moments is quite insensitive to rotation,[10] so that a mean-field approach based on a Heisenberg Hamiltonian is justified. The fairly successful (quantitative) reproduction of experimental data by our model justifies this point of view. A full itinerant treatment may possibly be a better approach to AF-F transitions in other intermetallic systems like, for instance, FeRh.[8]

*Present address: Max-Planck Institut für Metallforschung, D-70569 Stuttgart, Germany.

[1] R. B. van Dover, E. M. Gyorgy, and R. J. Cava, Phys. Rev. B **47**, 6134 (1993).

[2] J. H. V. J. Brabers, K. Bakker, H. Nakotte, F. R. de Boer, S. K. J. Lenczowski, and K. H. J. Buschow, J. Alloys Compd. **199**, L1 (1993).

[3] J. H. V. J. Brabers, A. J. Nolten, F. Kayzel, S. H. J. Lenczowski,

K. H. J. Buschow, and F. R. de Boer, Phys. Rev. B **50**, 16 410 (1994).
[4] J. H. V. J. Brabers, V. H. M. Duijn, F. R. de Boer, and K. H. J. Buschow, J. Alloys Compd. **198**, 127 (1993).
[5] N. Iwata, T. Ideka, T. Shigeoka, H. Fujii, and T. Okamoto, J. Magn. Magn. Mater. **54-57**, 481 (1986).
[6] A. Szytula, in *Handbook of Magnetic Materials 6*, edited by K. H. J. Buschow (North-Holland, Amsterdam, 1991), pp. 86–180.
[7] R. Radwanski and J. J. M. Franse, Handbook of Magnetic Materials 7, edited by K. H. J. Buschow (North-Holland, Amsterdam, 1993).
[8] J. S. Lord, P. C. Riedi, G. J. Tomkin, Cz. Kapusta, and K. H. J. Buschow, Phys. Rev. B **53**, 283 (1996).
[9] A. Hernando, J. M. Barandiaran, J. M. Rojo, and J. C. Gomez-Sal, J. Magn. Magn. Mater. **174**, 181 (1997).
[10] R. Coehoorn (private communication).